*Defect and Diffusion Forum Vols 188-190 (2001) pp 71-92*

*doi:10.4028/www.scientific.net/DDF.188-190.71*

# Atomistic Study of Diffusional Mass Transport in Metals

Yu.N.Osetsky

Materials Science and Engineering, Department of Engineering,
University of Liverpool. Liverpool L69 3BX,
UK

e-mail: osetsky@liverpool.ac.uk

**Keywords:** Diffusion, Atomistic Mechanism, Diffusion Coefficient, Correlation Factor, Random Walk, Migration Energy, Vacancy, Self-Interstitial Atom, Molecular Dynamics, Copper, Iron, Zirconium

**ABSTRACT.** Rigorous theoretical or phenomenological treatments of microstructure evolution in processes such as ageing or irradiation are based on particular mechanisms of mass transport, i.e. diffusion mechanisms. The information about such mechanisms is usually taken from simple theoretical models derived from experimental data. This works well in simple cases, but is limited in complicated situations like anisotropic diffusion, diffusion in alloys, etc., where the diffusion mechanism is not obvious. In the light of this, the atomic-scale molecular dynamics (MD) technique is a useful tool for identifying and studying actual mechanisms. In this paper we present the results of state-of-the-art MD studies applied to diffusional processes in bulk pure metals. We give a general formulation of the treatment of MD simulations of diffusion and discuss and compare methods to extract information about particular diffusion mechanisms. Examples of calculation of self-diffusion and defect diffusion coefficients and correlation factors, and treatment of diffusion mechanisms, are given for vacancy and self-interstitial atom diffusion in fcc, bcc and hcp metals. The cases of mass transport via small defect clusters (both vacancy and interstitial) are also discussed and examples are presented.

**List of acronyms:**

1D - one-dimensional;
3D - three-dimensional;
EAM - embedded atom model;
ESM - equivalent sphere method;
IAP - interatomic potential;
LRPP - long-ranged pair potential;
MBP - many-body potential;
MC - Monte Carlo;
MD - molecular dynamics;
MS - molecular statics;
MSD - mean square displacement;
RRT - residence requirement time;
RW - random walk;
SIA - self-interstitial atom;
TIM - two-interstitial model;
WSZ - Wigner-Seitz cell.

## 1. Introduction

Further progress in prediction and understanding of the properties of engineering materials under different conditions such as thermal treatment or irradiation demands an extended, multiscale approach where different stages are described with a maximum accuracy. Atomic transport via diffusion of point defects and their clusters is fundamental to microstructure change, and therefore property change, of any metal and alloy subjected to such conditions. Therefore the details of diffusion such as the mechanism and its parameters are the important input of any model, either

theoretical or phenomenological, aimed the prediction of materials behaviour. The very small scale involved, i.e. atomic size, makes this information difficult to obtain directly from experiment. The usual approach is to treat results of macroscopic experiments, e.g. self-diffusion of isotopes, impurity distribution near sinks, etc. within the appropriate diffusion theory using the mechanisms expected *a priori*. This works in some simple cases, but fails in more complicated situation when the diffusion mechanisms are not obvious. In these cases, atomistic modelling can provide valuable information on details of the process and parameters. The first attempts to use atomistic modelling in diffusion studies were made two to three decades ago [1–5] but were restricted in score by computer power. Recent progress in computer technology allows more sophisticated studies to be performed and new knowledge has been obtained on point defect diffusion mechanisms in pure metals [6–15], alloys [16,17] and near a dislocation [18]. Mass transport via defect clusters has also been investigated [12,14,19-24]. However, different authors use different techniques for atomistic data treatment and sometimes it is difficult to compare the results obtained even for the same metal. The description of treatment of diffusion simulation results is rather dispersed in the literature. In the present paper we try to collect this information and to give a description of the most successful techniques. This is accompanied by examples of molecular dynamics simulation of point defects diffusion in different structures.

The paper is organised as follows. In section 2 we present some basic features of atomistic methods and, in particular, molecular dynamics applied to the diffusion problem. In the next section some elements of atomistic theory of diffusion are given together with some methods for treating the data obtained from atomistic simulation. Some examples of point defect diffusion studies for different metals are reviewed in section 4. Mass transport via defect clusters is described briefly in section 5. This is followed in section 6 by summary of the main conclusions and views on some important problems related to diffusion and mass transport in metals.

## 2. Features of atomistic studies of diffusional mass transport.

Three atomic level methods are using in application to diffusional problems, namely molecular statics (MS), molecular dynamics (MD) and Monte Carlo (MC). Each method has its own limitations and advantages. Thus MS is used for estimation of migration energy by modelling the energy barrier along a diffusional path known *a priori*. This method is also used to study interactions of a defect with particular element of the microstructure, e.g. dislocations, to estimate the possible forces affecting the defect diffusion. MD simulates defect diffusion directly and allows investigation of diffusion mechanisms and estimation of dynamic properties of defects under both equilibrium and non-equilibrium conditions. MC is the method for a larger scale, which permits the study an effect of diffusion provided all the mechanisms, kinetic characteristics and interactions are known *a priori*. Among these methods only MD allows direct study of diffusion and therefore it is the main subject of the present paper. A short description of molecular dynamics techniques and the main features of their application to the study of diffusional transport now follows.

In MD a model crystallite consisting of atoms or molecules interacting via an appropriate potential is simulated. In the present paper we consider metallic systems where atoms interact via effective interatomic potentials (IAPs). The interatomic potential is the main physical input of any MD model and determines all the properties of the simulated system. For this reason IAPs are the subject of intensive study in solid state physics and a great number for different metallic systems have been constructed. The reader is referred to several original works in this area [25-27] while here we underline only that in MD studies interatomic potentials present effective interaction energy between atoms as a function of interatomic distances. This approximation, sometimes called 'classical MD', is based on classical Newtonian mechanics in contrast to 'first-principal MD' where

the simulated system consist of ions and valence electrons and all interactions between them are considered [28]. The latter allows more accurate description of the real physical system but at the moment it cannot be used in diffusion studies due to the huge computational resources required and therefore is not considered here.

The typical system for classical MD study of diffusion consists of $10^3$ to $10^5$ atoms simulated for a time up to a few tens of *ns*. Since only a small part of a real system is considered appropriate boundary conditions must be applied to simulate reaction with the rest of the system. Periodic boundary conditions are usually applied in MD studies of bulk diffusion.

The following steps are typical for study of thermally activated diffusional transport :

1. Construction of the model crystallite of appropriate crystal structure.
2. Creation of a defect. For example a vacancy is created by removal of an atom from the model crystallite while an interstitial defect is created by insertion of an extra atom in an appropriate configuration.
3. The force on every atom is calculated from its interaction with its neighbours. This allows relaxation of the crystallite to its ground or a metastable state. This is usually made by a static or quasi-dynamic technique to minimise the total potential energy and the forces on the atoms.
4. Heating of the model crystallite to the desired temperature by assigning to all atoms randomly distributed velocities, i.e. kinetic energy, with a mean equivalent to the temperature.
5. Integration of the equations of motion for all atoms to repeatedly update their velocity and position. A certain time is necessary to achieve an equilibrium phonon distribution and this time depends mainly on the temperature and may vary from few to few hundred *ps*. This period must be excluded from treatment of results. The value of the time step used in integration of the equations of motion must be sufficiently small for the atomic trajectories to be followed with accuracy and is typically of the order of *fs*, and therefore a typical MD simulation of a diffusion process involves $10^6$-$10^7$ integration steps.

Two features of the methodology for diffusion simulation should be mentioned.

The first is related to long simulation time necessary to generate a reasonable statistics of defect jumps. Tens of millions of time steps must be simulated without significant loss of accuracy. Since periodic boundary conditions are usually applied, i.e. constant volume, number of atoms and energy (microcanonical ensemble), the accuracy can be monitored by, for example, calculation of the crystallite temperature. To guarantee a constant mean temperature an integration scheme with a small time step must be applied. The velocity Verlet algorithm with a variable time step is rather stable for long time simulation [29, 30]. The criterion usually used to chose the value of time step $t_s$ is related to the velocity of the fastest atom $V_{max}$. The value of $t_s$ is recalculated every integration step from $t_s=d/V_{max}$, where $d$ is the maximum allowed displacement of the fastest atom. The value $d=0.0055$-$0.0065a$, where $a$ is the lattice parameter, satisfies the conditions for long-time simulation very well. The particular value of $t_s$ depends on the atomic velocity distribution which, in turns, depends on the interatomic potential, temperature and number of atoms in the crystallite, i.e. the bigger the crystallite the longer the tail of fast atoms in the velocity distribution function. An example of temperature evolution during the longest-ever published MD simulation of vacancy diffusion in hcp Zr [31] with many-body potential from [32] is presented in Fig.1. It can be seen that over about 70*ns* (which is equivalent to about $5\times10^7$ time steps) the change of mean crystallite temperature was negligible. The linear fitting resulted in the velocity of the temperature change equal to $0.5\times10^{-3}$ *K/ns*, which is certainly acceptable for this kind of simulation.

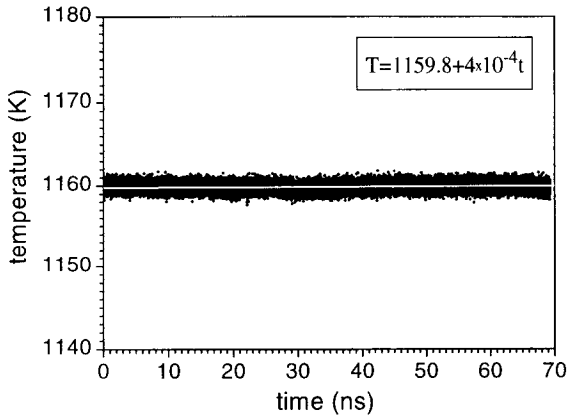


**Fig.1** Evolution of crystallite temperature during simulation of vacancy diffusion in hcp Zr. The white line indicates linear fitting of all data with the parameters indicated in the figure.

The second feature is related to the accumulation and localisation of long-time computing inaccuracy. We demonstrate this with an example of self-interstitial atom (SIA) diffusion in Cu simulated with a many-body potential from [25]. This simulation was made in a fcc crystallite of about 6000 mobile atoms and 2500 defect jumps were attained at each temperature [33]. The analysis of SIA jumps showed that there is a spatial correlation of jump frequency, for it is higher near boundaries than in the crystallite volume. By extracting data for a boundary layer of $1a$ thickness, e.g. two {100} planes, it is possible to separate the temperature dependence of the frequency 'volume' and 'boundary' jumps. The results are presented in Fig.2 where the difference can be clearly seen. This result is surprising at first sight because a periodic boundary is not a physical boundary. However, careful analysis has shown that this effect is related to the accumulation of computer inaccuracy due to extra calculations in construction of periodic boundaries at every time step. Any algorithm involving periodic boundaries requires translation of some atoms to include interactions with atoms across boundaries and therefore in calculating forces and energies of the atoms next to the 'periodic boundary' extra operations have to be performed. Although the operation inaccuracy is low (the typical inaccuracy for double precision floating-point operation is about of $10^{-15}$) it causes a permanent inward of inaccuracy from the boundary layer atoms, thereby creating a 'physical' boundary which may 'interact' with defects. The interaction energy is weak but it can be recognised at low temperatures. In addition, it is observed in [33] that at low temperature an SIA spends more time near boundaries than can be explained statistically, indicating that for this defect the 'interaction energy' is negative. One solution to this problem is the delocalisation and redistribution of the inaccuracy over the crystallite, for the inaccuracy itself is very small and the difficulty only arises because of its accumulation for boundary atoms. The technique we use is to keep the crystallite centre near the defect by periodic reassignment of boundaries, which can be done easily in any MD code. The results of using technique for the SIA simulation are presented in Fig.2 and the very good coincidence with the data for volume jumps can be seen.

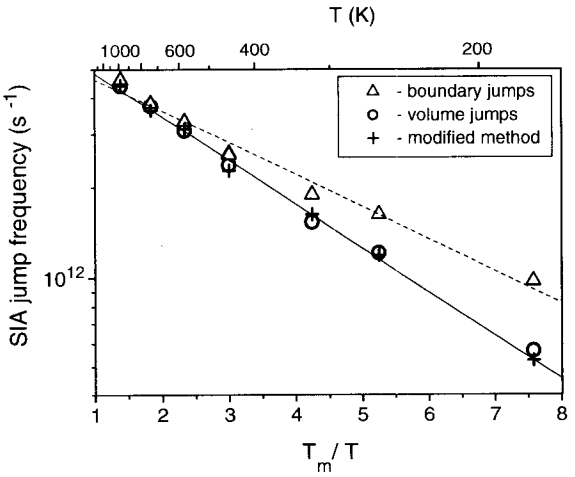


**Fig.2** Jump frequency versus the reciprocal temperature obtained for simulation of self-interstitial atom motion in Cu with the MBP. ($T_m$=1350K)

The impact of any diffusion simulation depends mainly on the quality of treatment which, in turn, depends on the information extracted during simulation. Successful simulation requires full monitoring of defects and extraction of information on atomic transport, energy distribution associated with defect, etc. Defect monitoring usually includes the position and configuration of a defect during all elementary processes. In most cases defect motion can be decomposed into a sequence of jumps and therefore information collected must include the time when each jump occurs and the direction, defect coordinates and configuration. In many cases the configuration of a defect can be changed, e.g. rotation of a self-interstitial without jump, and this information can be also extracted. The configuration analysis is usually based on analysis of all Wigner-Seitz cells (WSCs). When empty, the WSC is associated with a vacancy and a WSC with more than one atom is attributed to an interstitial type defect. An 'equivalent sphere' method (ESM) is sometimes used for defect monitoring. In this the space near each lattice site is divided into two enclosed spherical volumes with radii $R_V < R_{SIA}$. The analysis of the occupancy of sphere $R_V$ and spherical layer ($R_V$, $R_{SIA}$) allows identification of an atom at a lattice site (sphere $R_V$ includes an atom), a vacancy (no atom in $R_{SIA}$ sphere) and an interstitial (one or more atoms in $R_{SIA}$ sphere). The ESM involves a slightly simpler algorithm, but demands preliminary determination of $R_V$ and $R_{SIA}$, which are temperature dependent. One should also take into account that unlike the WSCs analysis, the ESM does not consider the whole interatomic volume and can therefore result in slightly different values of defect jump frequency (usually lower) and correlation factor (usually higher).

Molecular dynamics can provide a wide range of data for use in estimating diffusional parameters such as diffusion coefficients, migration energy, correlation factor and diffusion mechanisms, etc. A short description of methods of treating MD data based on atomic theory of diffusion follows.

## 3. Elements of theory of diffusion for application to atomistic study.

### 3.1 Diffusion coefficients.

We start from the Einstein equation, which is the basic equation in the theory of diffusion kinetics

$$D^* = \frac{<\vec{R}^2>}{6t} \tag{1}$$

where $D^*$ is the tracer diffusion coefficient in the simulated crystallite and $<\vec{R}^2>$ is the mean square displacement (MSD) of the tracer atoms

$$<R^2(t)> = \frac{1}{N_{tr}} \sum_{i=1}^{N_{tr}} \left[\vec{r}_i(t) - \vec{r}_i^{\,0}\right]^2 \tag{2}$$

where $\vec{r}^{\,0}$ and $\vec{r}_i(t)$ are initial and instantaneous positions of atom $i$ and $N_{tr}$ is the number of tracer atoms in the simulated crystallite. In practice, after a long enough simulation time (total simulation time will be denoted as $t_{MD}$ hereafter) $<R^2(t)>$ becomes a linear function versus time and the tracer diffusion coefficient $D^*$ can be obtained by fitting to the expression [30]

$$<R^2(t)> = A(t) + B + 6D^*t \tag{3}$$

where $\lim_{t_{MD}\to\infty}[A(t)]=0$ and $B$ is a temperature dependent constant (the MSD in the perfect crystal at the same temperature). Note that the thermal expansion of the crystallite has to be taken into account to ensure equilibrium conditions. This can be achieved by changing the lattice parameter to give a zero total pressure at each temperature [34]. The important feature of the definition of the self-diffusion coefficient via eq.3 is that it is not concerned with any particular diffusional mechanism.

More information can be obtained if the diffusion mechanism can be decomposed into a sequence of tracer atom jumps with the same length $\Delta$ of jump vectors $\vec{r}_i$ ($i=1...n_i$ and $n_i$ is a number of jumps) of the $i^{th}$ atom. Then MSD can be written as (see e.g. [35] for details)

$$<\vec{R}^2>=\frac{1}{N_{tr}}\sum_{k=1}^{N_{tr}}\left[\sum_{i=1}^{n_k}<\vec{r}_i^{\,2}>+2\sum_{i=1}^{n_k}\sum_{j=1}^{n_k-i}<\vec{r}_i\cdot\vec{r}_{i+j}>\right]=$$

$$=\frac{N^{jump}\Delta^2}{N_{tr}}\left[1+\frac{2}{N^{jump}}\sum_{k=1}^{N_a}\sum_{i=1}^{n_k}\sum_{j=1}^{n_k-i}<cos\Theta_{i,i+j}>\right] \qquad (4)$$

where $\Theta_{i,i+j}$ is the angle between the $i^{th}$ and $(i+j)^{th}$ jumps of the same tracer and $N^{jump}=\sum_{k=1}^{N_{tr}}n_k$ is the total number of jumps of tracer atoms. Substituting eq.(4) into eq.(1) another important expression of the atomic theory of diffusion can be obtained

$$D^*=f_{tr}\frac{\nu_a\Delta^2}{6}=f_{tr}\frac{\nu\Delta^2}{N_{tr}6} \qquad (5)$$

where the tracer correlation factor, $f_{tr}$, is defined by summation over cosines between all successive jumps of atoms

$$f_{tr}=\lim_{n_k\to\infty}\left(1+\frac{2}{N^{jump}}\sum_{k=1}^{N_{tr}}\sum_{i=1}^{n_k}\sum_{j=1}^{n_k-i}<cos\Theta_{i,i+j}>\right) \qquad (6)$$

and $\nu_a=\frac{N^{jump}}{N_{tr}\cdot t}=\frac{\nu}{N_{tr}}$ is the mean jump frequency of atoms and $\nu$ is the defect jump frequency. We have introduced defect jump frequency because this parameter is usually obtained in MD studies of point defect diffusion.

Hence, the two equations have been obtained which define the tracer diffusion coefficient in terms of the data obtained in simulation of defect diffusion for either mean squared displacements of all atoms or atom or defect jumps.

### 3.2 Correlation analysis.

Although eqs.1-6 are rather simple there are problems when applying them directly in MD simulation. They arises from the fact that in practice only few a thousand defect jumps can be simulated. This means that in a typical crystallite consisting of $N_a \approx 10^4$ atoms, each atom makes

less than one jump on average and only a small fraction of atoms exhibits more than one jump. Therefore atomic trajectories are too short to apply the above equations directly. However, due to the ergodicity hypothesis for independent events (e.g. atom jumps), the statistical properties of few long trajectories are the same as those of many short ones. In other words, all the atoms in MD can be assigned as tracers, i.e. $N_{tr} = N_a$ ($N_a$ is total number in the simulated crystallite) and eqs.1-3 can be applied straightforwardly. Although the trajectory of each particular atom is rather short the total MSD is a linear function which defines the self-diffusion coefficient unambigously. Examples of the temporal evolution of atomic MSD for the case of monovacancy diffusion in hcp Zr simulated in [31] with the MBP from [35] are presented in Fig.3. It can be seen that all the dependencies can be described well by a linear function which allows estimation of the self-diffusion coefficient to be performed with a high accuracy ($\delta < 1\%$).

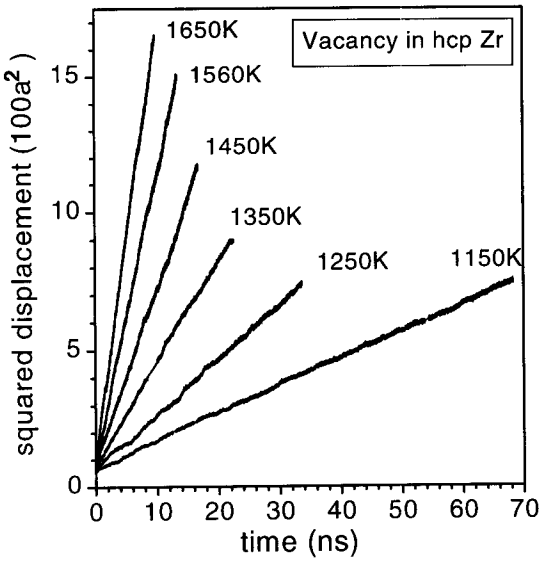


**Fig.3** Temporal evolution of atomic square displacements at different temperatures obtained by simulation of vacancy diffusion in hcp Zr.

However the tracer correlation factor cannot be estimated directly from eq.6. The general way to overcome this problem is to consider defect diffusivity. Actually all the Eqs.1-6 can be applied directly to a defect, with the only difference that in eq.5 $f_{tr}$ should be replaced by a defect correlation factor $f_d$ and $N_{tr}$ by the number of simulated defects, which in practice is usually equal to unity. Therefore the defect diffusivity $D^d$ can be written as

$$D^d = f_d \frac{\nu \Delta^2}{6} \tag{7}$$

where defect jump frequency ν is exactly the same as in eq.5 and $f_d$ can be obtained by eq.6 if $\Theta_{i,j}$ is defined as the angle between the $i^{th}$ and $j^{th}$ defect jumps. Note that the only approximation used here is that jumps of atoms and the defect are of the same length $\Delta$, which is valid for the majority of diffusion mechanisms. If the diffusion occurs via essentially isotropic random jumps of a defect in the absence of an extended force field, the expression for the defect correlation factor can be further simplified by a pair correlation approximation [35]. For example, for the vacancy mechanism it can be written as :

$$f_d = \frac{1+\overline{\cos\Theta}}{1-\overline{\cos\Theta}} \tag{8}$$

where $\Theta$ is the angle between two consecutive jumps of a defect, which can be easily obtained from MD simulation.

Sometimes in practical simulation there are problems in obtaining $f_d$ from analysis of jump direction. This occurs in the case on non-random walk of a defect (eq.8 cannot be used) or when only a single (or very few) defect trajectory is simulated (eq.5 cannot be used). The correlation analysis of eq.5, i.e. estimation of the correlation length, is possible but is sometimes inconvenient in practice. Another possible solution of this problem is the decomposition of a single defect trajectory into independent segments. The necessary conditions to apply this method are long enough trajectory (to include many segments) and long enough segments (to take into account the possible correlations). If the conditions are satisfied the defect diffusion coefficient is estimated as the average over diffusivities for each segment. Two similar realisations of this method have been used successfully in application to point defect diffusion. Thus in [2] the trajectory of a self-interstitial atom in tungsten was decomposed into segments of equal duration $\Delta t \approx 5\text{-}1000 ps$ whereas in [13,33] trajectories of the vacancy and SIA were decomposed into segments of an equal number of defect jumps $\Delta N_j$ = 5-20. In the both cases the final defect diffusion coefficient was estimated from global average over all segments, e.g. for isochronal distribution:

$$D^d = \frac{1}{N_s}\sum_{i=1}^{N_t}\left\{\frac{1}{n_s}\sum_{j=1}^{n_t}\frac{\vec{r}_{i,j}^{\,2}}{6\Delta t_i}\right\} \tag{8}$$

where $\vec{r}_{i,j}$ is the displacement vector of the $j^{th}$ segment in the $i^{th}$ series, $\Delta t_i$ is the duration of segments in the $i^{th}$ series, $N_s$ is the total number series with different $\Delta t_i$ and $n_s$ is the number of segments with $\Delta t_i$. It must be underlined here that to ensure the accuracy of the estimated defect diffusivity the convergence of diffusivity versus segment length must be analysed. To demonstrate this we present in Fig.4 the dependence of vacancy diffusion coefficient versus the duration of isochronal sequences, $\Delta t$, in Fe at T= $923K$ obtained by simulation with a long-ranged pair potential (LRPP) from [34]. The total number of jumps is 1000 and the diffusion mechanism is isotropic vacancy jumps. It can be seen that the diffusion coefficient saturates at $\Delta t > 75\ ps$. Note that the mean time delay between vacancy jumps in this simulation is $t_d \approx 24\ ps$ and therefore only decomposition into segments of $\Delta t > t_d$ makes sense. Note also that for a given trajectory the statistical inaccuracy increases for decomposition into longer segments. Therefore the compromise between the data inaccuracy and saturation of the results must be found.

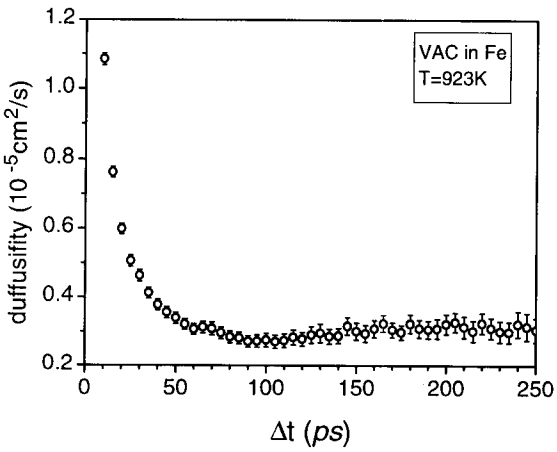


**Fig.4** Vacancy diffusion coefficient in α-Fe (simulated with the LRPP) versus duration of isochronal segments in decomposition of single vacancy trajectory simulated at 923K for 23*ns*.

Once defect diffusivity is estimated the tracer correlation factor can be obtained from

$$f_{tr} = \frac{D^*}{c_d D_d} = \frac{D_d^*}{D_d} \tag{9}$$

Here we take into account that all atoms in the simulated crystallite are tracers and introduce a self-diffusion coefficient per defect, $D_d^* = D^* / c_d$ ($c_d$ is defect concentration), because the defect diffusivity is also related to a single defect. For the particular case of defect random walk (RW), e.g. when $f_d = 1$, eq.9 can be simplified to

$$f_{tr} = \frac{< \vec{R}^2 >}{t \nu_{RW} \Delta^2} \quad . \tag{10}$$

### 3.3 Residence requirement time.

The RW case and eq.10 are often considered in theory because they are the basis of many theoretical, phenomenological and MC models used in practice. However it is necessary to discuss them here in more detail because the MD data are not obviously convertible into an RW mechanism, even when it actually occurs. Let us consider the simplest case of a bcc metal lattice where it is accepted that self-diffusion occurs via vacancy RW. In the first detailed study of vacancy diffusion in Fe [1] it was observed that there is a high probability that following a jump the vacancy performs a reverse jump after a short time delay, i.e. the first jump is unsuccessful. (We remember here that the jump frequency is the reciprocal of the jump time delay : $\nu = t_d^{-1}$). Such jumps increase the jump frequency and therefore $D_d$ in eq.7, but do not contribute to the diffusional transport. In order to correct the jump frequency the 'residence requirement time' (RRT) was introduced, characterised by a minimum time of stay, $t_{rr}$, for a jump to be successful and the constant empirical value $t_{rr} = 0.01$ps was used in [1]. Later, the concept of RRT was considered and extended in [13,17,33]. The RRT has a rather clear physical sense, underlining the fact that defect appearance in the next WSC does not necessarily mean that the act of migration has occurred. The defect must spend some time $\geq t_{rr}$ in the new site to be considered as resident in a new position. If a defect jumps back in a shorter time, as was observed in [1,13,33] the first jump is not 'real' but just a large fluctuation in atomic displacements. Using the word 'real' we emphasize that this and the previous jumps are not independent, contrary to what is assumed in RW model. Indeed, the vacancy correlation factor estimated in [11,33] for bcc Fe varied from 0.7 to 0.9 depending on the temperature. There are two possible reasons for this. One is related to features of lattice relaxation during defect jump. For example, the vacancy in the bcc structure in general is characterised by relatively large displacements. As discussed in [7], two types of phonon mode can be responsible for vacancy jumps in this lattice. The first is the high frequency $L\frac{2}{3}(111)$ mode and defines the frequency of jump attempts, whereas the other is the low frequency $T_1\frac{1}{2}(110)$ mode and is responsible for a specific relaxation of surrounding atoms. Therefore, not all the attempts can be successful but only those when the lattice has time to relax around the new position of the defect. If the surrounding atoms are insufficiently relaxed, the backward jump occurs. The other reason may be related to the method of defect monitoring in computer simulation and different methods might result in different distributions of forward and backward jumps and jump frequencies. In principle, there is no problem in correcting the jump frequency in any method of defect monitoring if one accompanies it with the corresponding defect correlation factor $f_d$. In this case the effective jump frequency, $\nu_{RW}$ , 'related' to RW can be defined as

$$\nu_{RW} = f_d \nu \tag{11}$$

The new frequency can be used in eq.10 to estimate the tracer correlation factor.

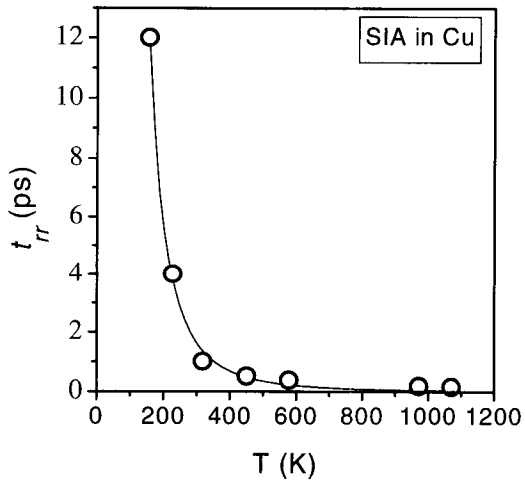


**Fig.5** Temperature dependence of the residence requirement time for the SIA defect in Cu obtained by fitting the jump statistics to a random walk.

The important impact of RRT is that its analysis can be used to estimate the cases when the random walk model can be applied. Thus in [13,33] $t_{rr}$ was used as a parameter to fit the jump frequency of the <100> dumbbell interstitial in Cu to the RW process. The method uses a variation of $t_{rr}$ to extract jumps (omitting pairs when a backward jump occurs within time < $t_{rr}$) which correspond to $f_d = 1$. The temperature dependence of $t_{rr}$ was obtained (see Fig.5) which, we believe, reflects the effective life-time of the phonons responsible for the mechanism studied. The jump frequency obtained, which is equivalent to $\nu_{RW}$, was used in eq.10 to estimate the tracer correlation factor $f_{tr}$ = 0.46±0.04, which is very similar to theoretical estimations $f_{tr}^{th}$ = 0.44 [36], thereby confirming that the mechanism studied is consistent with the RW.

In some cases the analysis of the RRT allows a new diffusion mechanism to be found, and an example will be presented in section 4.

### 3.4 Migration energy.

Once diffusion coefficients and jump frequencies at different temperatures $T$ have been obtained, the migration energy can be estimated using an Arrhenius dependence

$$D^*(T) = D_0^* \cdot exp\left(-\frac{E_m^*}{k_B T}\right) \tag{12a}$$

$$D^d(T) = D_0^d \cdot exp\left(-\frac{E_m^d}{k_B T}\right) \tag{12b}$$

$$\nu(T) = \nu_0 \cdot exp\left(-\frac{E_m^\nu}{k_B T}\right) \tag{12c}$$

where $D_0^*$, $D_0^d$ and $\nu_0^d$ are pre-exponential factors, $E_m^*$, $E_m^d$ and $E_m^\nu$ are the corresponding activation (migration) energies and $k_B$ is the Boltzmann constant. In eqs.(12) we omit the terms related to the migration entropy and assume that it is temperature independent and included in the pre-exponential factor.

In general, if the diffusion mechanism is unique and temperature independent, the migration energy obtained from eq.12a-c should be the same (provided all the equations describe the same process).

However, in many practical cases this is not so and the analysis of the difference in activation energies gives valuable qualitative information. The two following cases are possible :

1. The usual case is $E_m^* = E_m^d \neq E_m^v$. This happens when the estimated jump frequency ν is far from the corresponding $\nu_{RW}$. The analysis of defect correlation factor $f_d$ or residence requirement time $t_{rr}$ should clarify this difference.
2. The case $E_m^* \neq E_m^d$ is observed when the 'effective' tracer correlation factor $f_{tr}$ is temperature dependent. It is unlikely that $f_{tr}$ for a particular diffusion mechanism can be temperature dependent and therefore this case means that the diffusion mechanism is not unique and the contribution of the different mechanisms is temperature dependent. In this case the 'effective' tracer correlation factor is a combination of particular factors for each mechanism. Analysis of the defect configuration and migration mechanism at different temperatures could clarify this.

A comment should be made about the comparison of 'static', $E_m^{stat}$, and 'dynamic', $E_m^{dyn}$, migration energies. A 'static' migration energy is the potential energy barrier obtained by forcing an atom to move along a certain path which is supposed to describe a particular diffusion mechanism. This is usually done by repeated discrete displacements of an atom and relaxation of each instantaneous configuration but restricting displacements of the moving atom along the studied path (see e.g. [45]). In principle this method allows the minimum energy necessary to move an atom from one position to another to be estimated and in some cases this energy can be accepted as the minimum estimation of migration energy. Even in the most favourable case, when the dynamic diffusion mechanism is the same as that simulated statically, $E_m^{dyn} > E_m^{stat}$ due to thermal vibrations of atoms which increase the effective barrier. However, it is more often the case that the 'dynamic' path is not equivalent to the 'static' one or even that the diffusion mechanism is different. This situation usually occurs with interstitial atoms and in most cases $E_m^{dyn} < E_m^{stat}$. The reason for this is uncertainty in interstitial diffusion mechanism *a priori* when it is studied by the static technique. The same problem is also observed for vacancy diffusion when the displacements of atoms surrounding the defect are correlated. For example, this is the case for the 'double door' mechanism observed in the bcc lattice and investigated in [1,7] when $E_m^{dyn} < E_m^{stat}$.

## 4. Some examples of studies of diffusion by computer simulation.

### 4.1 Vacancy diffusion in bcc Fe.

Vacancy diffusion is the simplest case and in bcc Fe was studied in [1,11,14,17,33]. It was found that the vacancy exhibits isotropic jumps and all the treatment methods described in Section 2 can be applied successfully. As an example we present some results obtained in [11,33]. Vacancy diffusion was studied in a crystallite of about 4400 mobile atoms using a long-ranged pair potential [34]. The temperature range from 923K to 1573K was considered and from 1000 to 2000 vacancy jumps were treated at each temperature. Self-diffusion ($D^*$) and vacancy diffusion ($D^d$) coefficients, jump frequency, residence requirement time, tracer and defect correlation factors were studied. In Fig.6 we present Arrhenius plots for the $D^*$ and $D^d$ diffusion coefficients. Both dependences are linear and have the same slope, and therefore this is a case when the tracer correlation factor is temperature independent and $E_m^* = E_m^d$. The correlation factor was estimated via eq.9 as $f_{tr}$ = 0.72±0.03, which is consistent with the theoretical estimate for vacancy random walk in a bcc crystal $f_{tr}^{th}$ = 0.7272 [35]. The analysis of jump direction and time delay showed some

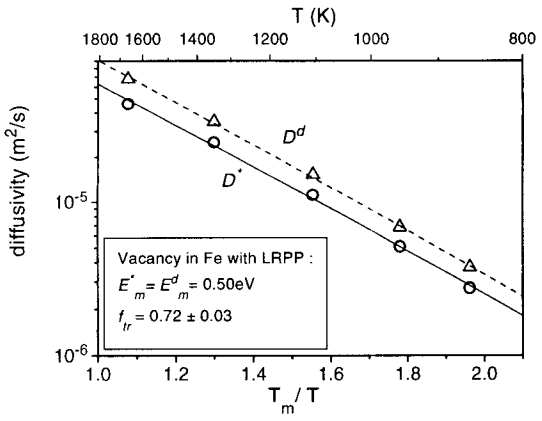


**Fig.6** Arrhenius plot for vacancy and self- diffusion coefficients obtained by simulation in α-Fe ($T_m$=1811K).

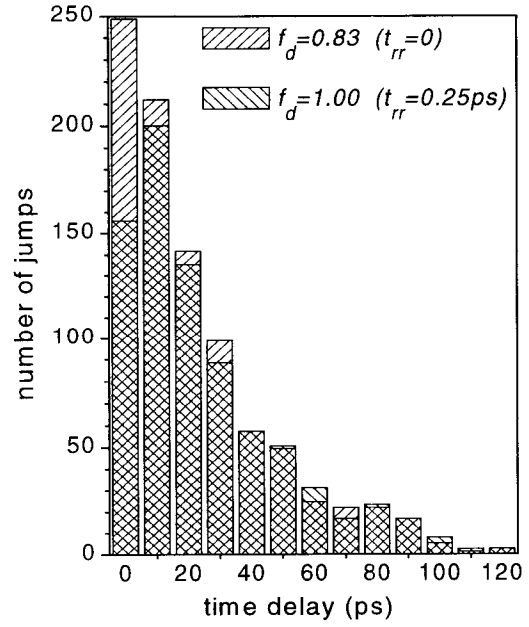


**Fig.7** Distribution of vacancy jump time delay obtained at 923K without residence requirement time analysis and with $t_{rr}$ = 0.25*ps* fitted to random walk.

peculiarities, however. Thus jumps treated with $t_{rr}$ = 0 had a large portion of fast backward jumps. This resulted in a vacancy correlation factor $f_d$ = 0.7 – 0.9, showing that vacancy jumps are not random in direction. However, the jump time delay has an exponential distribution, which is a feature of random events in time, e.g. see Fig.7 for T=923K. For the same temperature, the residence requirement time analysis shows that for $t_{rr}$ = 0.25 *ps* the vacancy correlation factor becomes equal to unity, i.e. isotropic random jumps in space, but the jump time delay is no longer exponentially distributed and shows a clear maximum at about 10*ps*, as can be seen in Fig.7 (note the mean time delay is equal to ≈24 *ps*).

### 4.2 Self-interstitial diffusion in bcc and fcc metals.

Self-interstitial atom diffusion has been studied quite intensively [1,2,8-15], especially in application to bcc metals and mainly for two reasons. The first, related to the interstitial mechanism in general, is due to the low migration energy of SIAs, which allows reasonable statistics of events (jumps) to be accumulated and, therefore, data of high accuracy to be obtained. The second arises from the commercial importance of bcc metals in nuclear industry, where the interstitial mechanism of mass transport is commonly accepted to be important. Different interatomic potentials have been used and the majority of studies have concluded that the diffusion mechanism of self-interstitial atom in bcc metals depends on temperature. At high temperature the dominant mechanism is via three-dimensional (3D) jumps of the <110> dumbbell while the contribution from one-dimensional (1D) jumps of the <111> crowdion increases at low temperature. Change in diffusion mechanism usually causes curvature of Arrhenius plots for diffusion coefficients and jump frequency, reflecting change of migration energy and correlation factor. In Fig.8 we present self-diffusion ($D^*$) and SIA diffusion ($D^d$) coefficients obtained in [13] with a many-body potential (MBP) for Fe [37]. Two features can be seen in Fig.8. One is the curvature of both plots, which reflects change in diffusion mechanism, and the other is the difference in effective migration

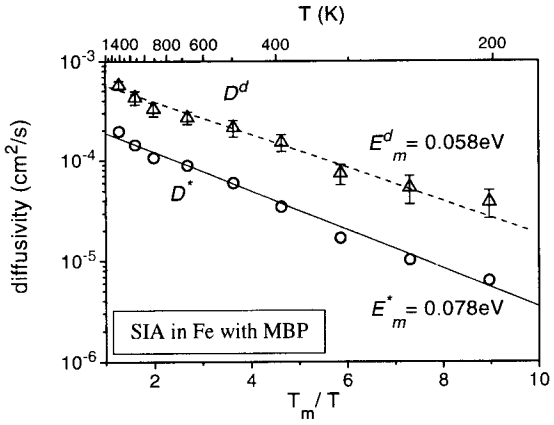


**Fig.8** Arrhenius plot for SIA and self- diffusion coefficients obtained by simulation of α-Fe with the MBP.

energy, e.g. $E^*_m \neq E^d_m$, which means that the tracer correlation factor is temperature dependent. The latter is also related to a temperature dependence of the diffusion mechanism. The temperature dependence of $f_{tr}$ is presented in Fig.9. The features of the diffusion mechanism at different temperatures were discussed in [13]. Thus, detectable diffusion starts only at T≈200K while at lower temperature the SIA is frozen in a <110> dumbbell configuration. For example at 150K SIA movement was not detected over a simulation time of about 5*ns*. At the temperature when the SIA starts to move, e.g. > 200K, the diffusion mechanism is rather complicated. In the temperature range 200-300K an SIA spends a significant time (10-350 *ps*) in a <110> dumbbell configuration followed by series of fast ($t_d$ = 0.05-0.50*ps*) jumps in one direction via the <111> crowdion mechanism (10-40 jumps). These are essentially random in a particular <111> direction and produce significant displacements contributing to self-diffusion. These features of low temperature diffusion are qualitatively similar to the multi-step mechanism discussed in [12] but with long series of crowdion jumps. When the temperature increases beyond this, the time SIA stays in a <110> configuration decreases and the number of <111> crowdion jumps (and therefore their contribution to diffusion) decreases. At high temperature the diffusion mechanism is be very close to 3D random jumps of a <110> dumbbell. The results of a statistical treatment of the contribution from the different types of jump are presented in Fig.9. Because of difficulties in such analysis, especially at high temperature when the SIA configuration is spread between the <110> dumbbell and <111> crowdion configurations (see e.g. [15]), these results should be taken as mainly qualitative. Nevertheless, the correlation between the value of $f_{tr}$ and the contribution from the <111> crowdion mechanism can be clearly seen. At high temperature $f_{tr}$ saturates at a value about 0.33 and this can be taken as the tracer correlation factor for the <110> dumbbell mechanism in a bcc metal lattice. Note that a similar value for this mechanism was also estimated in [14].

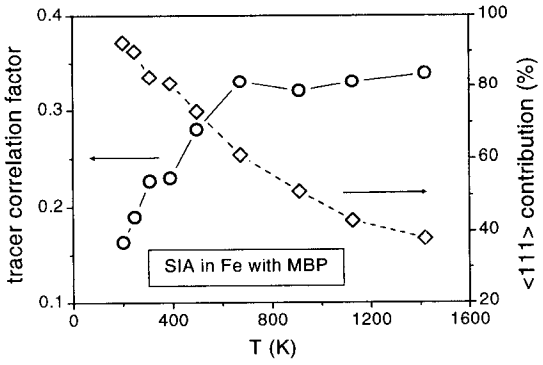


**Fig.9** Temperature dependence of the tracer correlation factor and contribution of <110> dumbbell jumps obtained by simulation of SIA diffusion in α-Fe with the MBP,

The quantification of contribution from different mechanisms and estimation of correlation factors depends very much on the interatomic potential used in simulation. The main factor is the relative stability of different SIA configurations, particularly the <110> dumbbell and <111> crowdion, for a given potential. For example, for a model based on the LRPP used in [13], the <111> crowdion is the stable SIA configuration, resulting in a larger crowdion contribution and lower values of $f_{tr}$ ($f_{tr}$ =

0.02-0.12 for T=300-1450K). A qualitatively similar temperature dependence of the contributions of the dumbbell and crowdion mechanisms to SIA diffusion in Fe was obtained in [11,15] with the well-known Johnson potential [38] and an embedded atom model (EAM) potential respectively. Analysis has shown that the relative stability of SIA configurations in a bcc metal lattice depends on the range of interatomic potential used, such that the longer range tends to stabilise the <111> crowdion (see e.g. [39,40]).

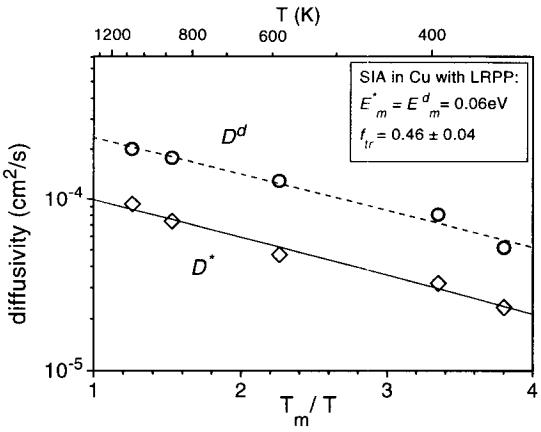


**Fig.10** Arrhenius plot for SIA and self- diffusion coefficients obtained by simulation in fcc Cu with the LRPP.

SIA diffusion in a fcc metal structure was studied in [13,33] and, again, some difference in results was found for different potentials. Thus the LRPP for Cu [34] simulates 3D isotropic diffusion via <100> dumbbell mechanism over the temperature range 350-1073K. An example of the temperature dependence of $D^*$ and $D^d$ is presented in Fig.10. Both plots are parallel, which means $E^*_m = E^d_m$ and the mechanism can be presented as random walk with a corresponding value of tracer correlation factor (see discussion on RRT in section 3.3 and Fig.5). Application of a MBP for Cu [25] yielded a more complicated picture of SIA diffusion. Thus the SIA correlation factor $f_d$ was found to be >1 at high temperature and <1 at low temperature. The RRT and configuration analyses resulted in three diffusion mechanisms. The dominant mechanism at all temperatures was found to be 3D diffusion of the <100> dumbbell. At high temperature fast jumps via <110> crowdions were observed and contributed up to 10% of total jumps. At low temperature a rather complicated motion of interstitial atom occurs and, based on RRT analysis, was interpreted as a <100> crowdion mechanism (see [13] for details). The Arrhenius plots of $D^*$ and $D^d$ presented in Fig.11 result in different migration energies and a temperature dependent tracer correlation factor which varies from 0.18 to 0.53 in the temperature range 132-976K.

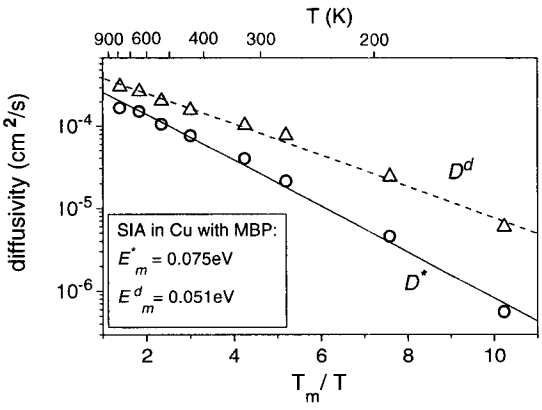


**Fig.11** Arrhenius plot for SIA and self- diffusion coefficients obtained by simulation in Cu with the MBP.

Note that the plot for the self-diffusion coefficient in Fig.11 is curved and shows a decrease of effective migration energy at high temperature, which can be explained by a contribution from the low-barrier <110> crowdion mechanism. It is interesting to compare this with the opposite curvature of the $D^*(T)$ plot for Fe (see Fig.8), where an increase of the effective migration energy at high temperature is explained by a decrease of the contribution from the low-barrier <111> crowdion mechanism.

### 4.3 Diffusion in anisotropic structures.

Diffusion in anisotropic materials is important in many applications for fuel and construction materials used in nuclear energy generation, but has not been widely studied as far as direct simulation of diffusion mechanisms is concerned. A number of investigations have considered point defect structure, migration paths and barriers in hexagonal closed packed (hcp) metals by static simulation [41-45] whereas the only two studies [10,15] have been devoted to dynamics of diffusion via the interstitial mechanism and the author is not aware of any published MD study of vacancy mechanism.

Vacancy and SIA diffusion in a model hcp metal has been studied recently [31] in crystallite consisting of about 6000 mobile atoms interacting via a many-body potential for Zr obtained in [34]. Much attention was paid to the statistical properties of the results obtained. For SIA diffusion 15,000 jumps were simulated at each of nine temperatures in the range 150-1600K. In the case of a vacancy the number of simulated jumps varied from 1,000 to 2,000, which required up to about 70 *ns* for the lowest temperature studied. In total six temperatures from 1150K to 1650K were simulated for the vacancy and for the four lowest temperatures two independent runs were performed. The total time simulated in the study of vacancy diffusion was about 0.3 μ*s*, which is equivalent to about 220,000,000 time steps. Such a long-time simulation allowed statistically significant results on diffusional parameters to be obtained. A detailed description is in [31] : here we summarize the main results and conclusions.

The SIA diffusion mechanism was found to be temperature dependent. At low temperature (<250K) a purely 1D mechanism via a $<11\bar{2}0>$ crowdion was observed. Higher temperature causes crowdion rotation in and off the basal plane. The frequency of rotation strongly depends on temperature with a significant preference for in–plane rotation. Therefore, in the temperature range 300-1000K the main mechanism can be described as planar (2D) diffusion in a basal plane with occasional changes of the particular {0001} plane. At higher temperatures the frequency of off–plane jumps quickly increases, but remains lower than that of $<11\bar{2}0>$ jumps or in–plane rotation. Qualitatively similar results for the temperature dependence of the SIA diffusion mechanism were reported earlier [10,15].

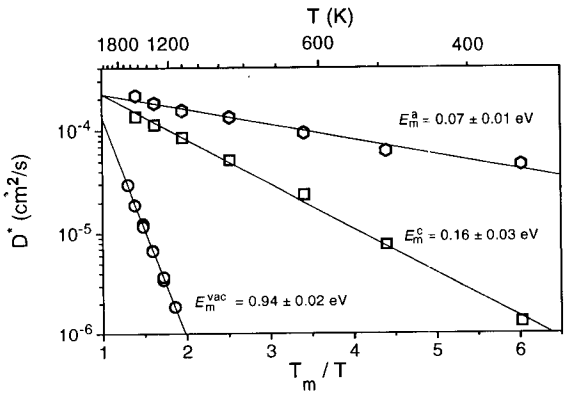


**Fig.12** Arrhenius plot for the self-diffusion coefficient for the vacancy mechanism and the in-plane and off-plane contribution to self-diffusion via the SIA obtained by simulation in hcp Zr.

Diffusion by the vacancy mechanism was found to be isotropic within the accuracy obtained. Although the number of in–plane jumps was systematically observed to be larger than that of off–plane jumps (by an average of about 10%), the diagonal elements of the matrix of self-diffusion coefficients were found to be equal. This result is rather surprising because the static potential energy barrier obtained for the in-plane path (0.84eV) was found to be lower than that for the off–plane path (0.89eV). A possible explanation may be found in analysis of correlation factors for the in–plane and off–plane mechanisms. The study of this is in progress and the results will be published elsewhere.

The temperature dependence of the self-diffusion coefficients of the vacancy and of the SIA for the in– and off–plane mechanisms are presented in Fig.12. The vacancy migration energy obtained from the data is slightly higher than the static barrier value. The migration energy for the SIA off–plane mechanism is more than double that for the in–plane mechanism. Also, both the SIA plots exhibit curvature. The in–plane diffusion plot curves towards a higher migration energy at high temperature whereas that of the off–plane plot curves towards a lower energy in such a way that the plots do not intersect.

## 5. Special cases of mass transport.

### 5.1. Diffusion at high vacancy concentration.

An interesting result was obtained in [46] where the diffusion in a vacancy-rich zone (reproducing the central region of a high energy displacement cascade) in Fe was studied by MD. It was found that at high vacancy concentration (5-15at%) very mobile dispersed vacancy clusters were formed. The mobility of vacancies within these clusters was much higher than that in the bulk and the effective migration energy could decrease by up to a few times. It is important to note that the decrease of effective migration energy is not explained by a lower energy barrier along the diffusion path, for that was found to be similar to that for a vacancy in the bulk [46]. A qualitatively similar result was also obtained in a study of 2at% vacancy population within coherent bcc Cu precipitates in a bcc Fe matrix [17]. MD study has demonstrated that such an effect exists for much lower vacancy concentrations. Thus in [47] diffusion by the vacancy mechanism in periodic bcc Fe crystallites was studied. Crystallites with a different number of vacancies were simulated : single vacancy in crystallites containing 250, 432 and 1024 lattice sites and five vacancies uniformly distributed in crystallites of 1024 and 2000 sites, corresponding to averaged vacancy concentrations of 0.4, 0.2, 0.1, 0.5 and 0.3at%, respectively. All simulations were performed at 900K and the self-diffusion coefficient was estimated. The results for the single vacancy showed a weak increase of $D^*$ with increasing crystallite size (at about 15% for 1024 atoms in comparison with 250 atoms). This can be explained by a change in phonon spectrum (the larger the crystallite the lower the frequency of phonons that can be simulated) and in velocity distribution (the larger the crystallite the longer the tail of fast atoms in the velocity distribution). The simulation of five vacancies resulted in a diffusion coefficient (normalised to the number of vacancies) of up to more than twice that for a single vacancy. Since vacancies never approached closer than 3a to each other, this effect cannot be explained by a simple defect mechanism such as formation and movement of a di-vacancy. The following conclusion may be drawn. Interactions between multiple vacancies are recognisably stronger than the interaction between a vacancy and its image in periodic crystallites. This interaction causes a significant increase in vacancy jump frequency and diffusivity. A clear understanding of this effect has not yet been achieved, but a possible explanation presented in [46] is based on the effect of a vacancy population on the local distribution of phonons. Dynamic interaction between vacancies in a dispersed cluster lowers the frequency of the $T_1\frac{1}{2}(110)$ phonon mode, which causes an increase of vacancy jump frequency. Such long-range dynamic interactions between defects could be important for defect kinetics in conditions where local fluctuations of defect density exist. For example, recent positron annihilation studies of irradiated Fe have detected a rather high population of small vacancy clusters (40-50 vacancies), invisible in a transmission electron microscope [48]. Note that in a similar MD study of a vacancy population in fcc Cu, a similar fast diffusion of vacancies was observed but it resulted in clustering and formation of compact immobile vacancy clusters of stacking fault tetrahedron type [39]. This difference in behaviour can be understood if one takes into account the significantly higher binding energy of compact vacancy clusters in fcc metals.

### 5.2 Thermally-activated mass transport via interstitial clusters.

Most current descriptions of microstructure evolution in metals under cascade producing irradiation are based on the production bias model [49] and stress the importance of the glissile SIA clusters produced directly in high energy displacement cascades [50]. These clusters may be responsible for high swelling and swelling heterogeneity at low irradiation doses [49], formation of specific microstructures like rafts of dislocation loops [51], decoration of dislocations by dislocation loops [52], void lattice formation [53] and be the cause of specific behaviour under deformation such as localisation of plastic deformation, known as channelling [54]. The realisation of the possible importance has led to extensive atomistic studies of the structure and dynamic properties of such clusters [12, 13, 19-24, 39, 55-57]. These simulations have shown that glissile SIA clusters consist of parallel crowdions aligned along a closed packed crystallographic direction. In terms of the dislocation description of extended defects, such clusters are described as perfect edge dislocation loops. The most important feature of such clusters is that their motion can be thermally activated without the need for applied stress. A number of MD studies of models of bcc [12,19-24,56], fcc [19,20,23,57] and hcp [56] metals has proved that clusters having up to few hundred SIAs (i.e. up to ≈3-4 *nm* in diameter) exhibit very fast one-dimensional motion. Attempts have been made to describe such motion and the corresponding mass-transport within the diffusional approximation wherein a jump is defined as a displacement of the cluster centre of mass by the lattice vector along the close packed direction of motion. The effective migration energy deduced from the jump frequency analysis is found to be size independent and similar to that of an isolated single crowdion of the same type, whereas the jump frequency decreases with increasing cluster size [19,23,57] (see for example Fig.13 for SIA clusters in Fe simulated with the LRPP). A similar glide process was also found to occur with perfect vacancy clusters [22]. Another interesting feature of cluster behaviour is that they can exhibit continuous motion (jumps, glide) in the same direction over a long distance $>>a$, e.g. up to 12 *nm* at low temperature [57]. Using diffusional language this can be described as a strongly correlated process. Detailed study of the SIA cluster glide mechanism has shown that motion of a cluster centre of mass occurs via jumps of its consistent crowdions that are independent in time and correlated in direction [19,21]. However, a clear understanding of this phenomenon is not yet achieved and new approaches must be developed.

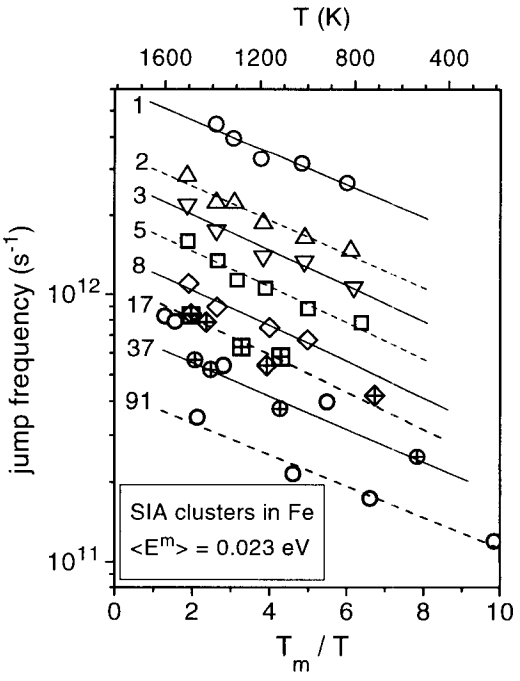


**Fig.13** Jump frequency of SIA clusters in bcc Fe versus the reciprocal temperature obtained with the LRPP.

It must be underlined here that the case of one-dimensional diffusion is very difficult for treatment, even in the case of point defects. The examples presented above of SIA diffusion in bcc and hcp metals have already pointed to this problem. The key to this lies in the specific structure of defects that exhibit 1D motion. So far, this was observed only for crowdion-like defects. It is unlikely that this type of defect can be considered as a point defect because of the

extended range of atomic displacements along the crowdion line. The deformation is extended for tens of lattice parameters away from the crowdion centre [22,58]. Such delocalised defects must be very sensitive to long wave vibrations (phonons) in crystals and this may result in specific properties like low effective migration energy (lower than the average thermal energy of atoms in the crystal), strong correlations in motion and strong interactions with other microstructural features. Although the general reaction kinetics applied to one-dimensional diffusion have already been developed [59], the treatment is based on 1D random walk of a localised defect, and this does not describe the case of 1D glissile defect clusters and, most probably, not even the single crowdion.

## 6. Contribution of atomistic simulation to understanding of defects behaviour.

Intensive and rigorous MD studies of defect dynamics in metals can clarify many questions and uncertainties concerning their behaviour under different conditions. For example, the well-known 'two-interstitial model' (TIM) was suggested to resolve some problems in the kinetics of development and annealing of damage in irradiated metals [60]. The main supposition of the TIM is that the self-interstitial atom can contribute to transport via two different states, i.e. a relatively slow ground state (dumbbell) and very fast metastable or 'exited' state (crowdion). This was proved by simulation of the SIA in bcc [3,8,9,11-13] and fcc [13] and hcp [10,15,31] metals. Although the simulation results are sensitive to various degrees to the interatomic potentials employed, the possibility of the TIM being valid in principle was clearly demonstrated. The related problem is considered in [58] for annealing of electron irradiated Cu. In order to describe the kinetics of electrical resistivity recovery, one-dimensionally migrating di-interstitials were introduced. MD simulations of SIA clusters in Cu have demonstrated that in low-temperature motion of the smallest clusters, e.g. di-interstitials, the one-dimensional <110> crowdion mechanism dominates [13,56].

The importance of SIA clusters in the creation of specific microstructures in irradiated metals was mentioned in section 5.2. It should be noted that the dynamic properties of glissile clusters revealed by atomistic modelling have confirmed the basic ideas of the production bias model which allows many experimental observations to be understood. As an example, consider the inhomogeneity of irradiation-induced void swelling in metals. It was found that in neutron-irradiated metals such as V, Nb, Cu, Al and Ni, the accumulation of vacancies in the form of voids is significantly enhanced in a wide zone known as 'peak zone'. The 'peak zone' is of width ~3-6$\mu m$ and located between the defect-free region, in the vicinity of grain boundary ('denuded zone' of width ~100$nm$), and the region in the grain interior with a significantly lower constant swelling (see [61] and references cited). Explanation of such microstructure [61,62] is based on long-range one-dimensional glide of the SIA clusters formed in displacement cascades considered in section 5.2. The same feature of SIA clusters can also be used in explanation irradiation creep in cubic materials and together with highly anisotropic diffusion of single SIAs in the hcp lattice (see section 4.3) can be used for explanation of radiation creep and growth of anisotropic materials.

## 7. Conclusions and scope for future studies

The comparison of data obtained with different interatomic potentials has shown that important properties of point defects, e.g. their migration mechanism, can be sensitive to interatomic potentials used. Therefore, in every particular study attention should be paid to the choice of an appropriate interatomic potential.

The examples of point defect diffusion in pure metals presented in section 5 have demonstrated that this case can be successfully studied if an appropriate and rigorous analysis of atomic data is applied via extended MD simulation. In many cases static simulation is not able to predict defect characteristics, e.g. the migration energy and mechanism, and full molecular dynamics simulation must be performed.

While diffusion processes in pure metals have now been studied fairly widely and a considerable amount of information has been obtained, the understanding of diffusion mechanisms in alloys is in its infancy. A few full MD investigations, for example of binary [16, 17] and ordered [63] alloys, have shown that the diffusion mechanisms may be complicated but can be treated successfully. This case must be considered in more detail and different types of alloys, random and ordered, dilute and concentrated, substitutional and interstitial, etc., should be simulated to provide information on diffusion mechanisms and parameters necessary for realistic prediction of materials behaviour.

Another important subject is defect diffusion in materials under stresses. Diffusion occurs under stresses in many real situations, whether from internal microstructure like dislocations, boundaries and interfaces, lattice defects, etc. or from loads applied externally. Although general theories of diffusion under stress have been developed [35,36], they are based on rather simple models and there is a lack of detailed, atomic level information of defect behaviour under such conditions. This is another topic that can be tackled by computer simulation.

**Acknowledgements**

Thanks are due to Prof. D.J.Bacon, Prof. A.Lidiard, Prof. A.Serra and Dr. A.V.Barashev for numerous discussions. The author also acknowledges the award of a Research Fellowship by the University of Liverpool.

**REFERENCES**

[1] D.H.Tsai, R.Bullough and R.C.Perrin, J.Phys.C: Solid State Phys., 3 (1970), p. 2022.
[2] C.H.Bennett, Thin Solid Films, 25 (1975), p. 65.
[3] M.W.Guinan, R.N.Stuart and R.J.Borg, Phys.Rev., B15 (1977), p. 950.
[4] A.Da Fano and G.Jacucci, Phys. Rev. Lett., 39 (1977), p. 950.
[5] G.De Lorenzi, G.Jacucci and V.Pontikis, Surf. Sci., 116 (1982), p. 391, G.De Lorenzi and F.Ercolessi, Europhys Lett., 20 (1992), p. 349.
[6] F.Willaime and C.Massobrio, Phys. Rev., B 43 (1991), p. 11653.
[7] A.G.Mikhin and Yu.N.Osetsky, J.Phys.: Condens. Matter., 5 (1993), p. 9121.
[8] T.Harry, Ph.D. Thesis, University of Liverpool (1998).
[9] A.M.Minashin and V.A. Ryabov, J. Nucl. Mater., 237 (1996) p. 996.
[10] B.J.Whiting and D.J.Bacon, Mat. Res. Soc. Symp. Proc., 439 (1997), p. 389.
[11] Yu.N.Osetsky and S.Serra, Defects and Diffusion Forum, 143-147 (1997), p. 155.
[12] B.D.Wirth, G.R.Odette, D.Maroudas and G.F.Lucas, J.Nucl.Mater., 244 (1997), p.185.
[13] Yu.N.Osetsky, A.Serra, V.Priego, F.Gao and D.J.Bacon, Mat. Res. Soc. Symp. Proc., 527 (1998), p. 69.
[14] N.Soneda and T.Dias de la Rubia, Philos. Mag., A 78 (1998), p. 995.
[15] R.C.Passianot, A.M.Monti, G.Simonelli and E.J.Savino, J.Nuc.Mater., 276 (2000), p. 230.
[16] Yu.N.Osetsky, A.Serra and S.I.Golubov, Defects and Diffusion Forum, 143-147 (1997), p. 505.

[17] Yu.N.Osetsky and A.Serra, Philos. Mag., A75 (1997), p. 1097.
[18] J.Huang, M.Meyer and V.Pontikis, Phys. Rev., B 42 (1990), p. 5495; Philos. Mag., A 63 (1991), p. 1149.
[19] Yu.N.Osetsky, A.Serra and V.Priego, Mat. Res. Soc. Symp. Proc., 527 (1998), p. 59.
[20] Yu.N.Osetsky, D.J.Bacon and A.Serra, Mat. Res. Soc. Symp. Proc., 538 (1999), p. 649.
[21] A.V.Barashev, Yu.N.Osetsky and D.J.Bacon, *Ibid,* 540 (1999), p. 697, ; Philos. Mag.,(2000) in press.
[22] Yu.N.Osetsky, D.J.Bacon and A.Serra, Philos.Mag.Lett.79 (1999), p. 273.
[23] Yu.N.Osetsky, D.J.Bacon, A.Serra, B.N.Singh and S.I.Golubov, J.Nucl.Mater., 276 (2000), p. 65.
[24] B.D.Wirth, G.R.Odette, D.Maroudas and G.E.Lucas, *Ibid*, p. 33.
[25] M.W.Finnis and J.E.Sinclair, Philos. Mag., A 50 (1984), p. 45, G.J.Ackland, G.Tichy, V.Vitek and M.W.Finnis, Philos. Mag., A56 (1987), p. 735.
[26] M.S.Daw, S.M.Foiles and M.I.Baskes, Mat.Sci.Reports, 9 (1983), p. 251.
[27] J.A.Moriarty, Phys. Rev., B 42, (1990), p. 1609; X.Y.Liu, J.B.Adams, F.Ercolessi and J.A.Moriarty, Model. and Sim. in Mat. Sci. and Eng., 4, (1996), p. 293 ; J.A.Moriarty, W.Xu, P.Soderlind, J.Belak, L.H.Yang and J.Zhu, J. of Eng. Mat. and Tech. Trans. ASME, 121, (1999), p. 120.
[28] R.Car and M.Parinello, Phys. Rev. Lett., 55, (1985), p. 2471.
[29] D.Frenkel and B.Smit, Understanding Molecular Simulation : from algorithms to applications, Academic Press 1996.
[30] D.Fincham in: *Dynamical Processes in Condensed Matter, Adv. Chem. Phys.*, LXIII, ed. M.W.Evans (Wiley, NY), 1985, p.493.
[31] Yu.N.Osetsky, D.J.Bacon and N.De Diego, (2000), to be published.
[32] G.J.Ackland, S.J.Wooding and D.J.Bacon, Philos. Mag., A 71 (1995), p. 553.
[33] Yu.N.Osetsky and A.Serra, (1997) unpublished.
[34] Yu.N.Osetsky, A.G.Mikhin and A.Serra, Philos. Mag.,A 72 (1995), p. 361.
[35] J.R.Manning, Diffusion Kinetics for Atoms in Crystals, D.Van Nostrand Company (Canada, Toronto), 1968.
[36] A.R.Allnatt and A.B.Lidiard, Atomic Transport in Solids, Cambridge University Press 1993, p. 359.
[37] G.J.Ackland, D.J.Bacon, A.F.Calder and T.Harry, Philos.Mag., A 75 (1997), p. 713.
[38] R.A.Johnson, Philos. Mag., 16( 1967), p. 533.
[39] Yu.N.Osetsky, M.Victoria, A.Serra, S.I.Golubov and V.Priego, J. Nucl. Mater., 251 (1997), p. 34.
[40] G.Simonelly, R.Passianot and E.J.Savino, Mat. Res. Soc. Symp. Proc., 291 (1993), p. 567.
[41] R.A.Johnson, Philos. Mag., A 63 (1991), p. 865.
[42] J.R.Fernandez, A.M.Monti and R.C.Passianot, J. Nucl. Mater., 229 (1996), p. 1.
[43] A.M.Monti, Phys. Stat. Sol., b 167 (1991), p. 37; R.C.Passianot and A.M.Monti, J.Nuc.Mater., 264 (1998), p. 198.
[44] D.J.Bacon, J.Nucl.Mater., 159 (1988), p. 176; *Ibid* 206 (1993), p. 249.
[45] A.G.Mikhin, Yu.N.Osetsky and V.G.Kapinos, Philos. Mag., A 70 (1994), p. 25.
[46] V.G.Kapinos, Yu.N.Osetsky and P.A.Platonov. J. Nucl. Mater., 184 (1991), p. 211.
[47] Yu.N.Osetsky, (1996), unpublished.
[48] M.Eldrup and B.N.Singh, J.Nucl. Mater., 276 (2000), p. 269.
[49] C.H.Woo and B.N.Singh, Philos. Mag., A 65 (1992), p. 889; B.N.Songh and A.J.E.Foreman, *Ibid*, A 66 (1992), p. 975; B.N.Singh, S.I.Golubov, H.Trinkaus, A.Serra, Yu.N.Osetsky and A.V.Barashev, J. Nucl. Mater., 251 (1997), p.107; S.I.Golubov, B.N.Singh and H.Trinkaus, *Ibid*, 276 (2000), p. 78.

[50] A.J.E.Foreman, C.A.English and W.J.Phythian, Philos. Mag., A 66 (1992), p.655; D.J.Bacon, F.Gao and Yu.N.Osetsky, Proc. COSIRES-98, Nucl. Instr. And Meth., B 153 (1999) p. 87; J.Nucl. Mater., 276 (2000), p. 1.
[51] J.O.Stiegler and E.E.Bloom, Rad. Effects, 8 (1971), p. 33; B.N.Singh, A.Horsewell, P.Toft and D.J.Edwards, J. Nucl. Mater. 224 (1995), p. 131.
[52] J.L.Brimhall and B.Mastel, *Radiat.Eff.* 3 (1970), p. 325; B.N.Singh, J.H.Evans, A.Horsewell, P.Toft and D.J.Edwards, J. Nucl. Mater. 223 (1995) 95; B.N.Singh, J.H.Evans, A.Horsewell, P.Toft and G.V.Müller, J.Nucl.Mater. 256-263 (1998), p. 865.
[53] A.J.E.Foreman, Harwell Report, AERE R-7135 (1972); P.Hähner and W.Frank, Solid State Phenomena, 23-24 (1992), p. 203.
[54] B.N.Singh, A.J.E.Foreman and H.Trinkaus, J.Nucl.Mater., 249 (1997),p. 91; *Ibid,* p.103; *Ibid,* 251 (1997), p. 172; N.M.Ghoniem and B.N.Singh, Proc. Of 20th Risø Int. Symp. on Materials Science : *Deformation-Induced Microstructures : Analysis and Relation to Properties*, Eds: J.B.Bilde-Sørensen *et al.*, Risø National Laboratory, Roskilde, Denmark, (1999), p. 41.
[55] Yu.N.Osetsky, A.Serra, B.N.Singh and S.I.Golubov, Philos. Mag., A 80 (2000), p. 2131.
[56] N.De Diego, Yu.N.Osetsky and D.J.Bacon, to be presented in MRS Fall meeting (2000).
[57] Yu.N.Osetsky, D.J.Bacon, A.Serra, B.N.Singh and S.I.Golubov, to be submitted to Philos. Mag., A (2000).
[58] E.Kuramoto, J.Nucl. Mater., 276 (2000), p. 143.
[59] W.M.Lomer and A.H.Cottrell, Philos. Mag., 46 (1955), p. 711.
[60] A.Seeger, in : Radiation Damage in Solids, Vol.1, IAEA, Vienna (1962), p.101; W.Frank and A.Seeger, Cryst.Latt.Defects, 5 (1974), p. 141.
[61] H.Trinkaus, B.N.Singh and A.J.E.Foreman, J.Nucl.Mater., 199 (1992), p. 1.
[62] B.N.Singh, Rad. Effects and Defects in Solids, 148 (1999), p. 383.
[63] J.Duan, Yu.N.Osetsky and D.J.Bacon, Defects and Diffusion Forum, (2000), to be published.

**Defects and Diffusion in Metals**
10.4028/www.scientific.net/DDF.188-190

**Atomistic Study of Diffusional Mass Transport in Metals**
10.4028/www.scientific.net/DDF.188-190.71